PREDICTION OF STIFFENER-SKIN SEPARATION IN COMPOSITE PANELS[1]

Han-Pin Kan
Mary A. Mahler
Ravi B. Deo

Northrop Corporation
Aircraft Division
Department 3853/82
One Northrop Avenue
Hawthorne, California

ABSTRACT

A methodology has been developed to predict the failure of stiffened composite panels by stiffener-skin separation. The methodology is applicable to curved or flat panels under combined uniaxial compression and in-plane shear loads. The analytical crux of the methodology are two analysis packages: (1) PACL1 which predicts the stress and displacement fields in a stiffened postbuckled panel and (2) WEBSTER, which predicts the local interfacial (shear and normal) stresses at the skin and stiffener flange junction. PACL1 is a Rayleigh-Ritz analysis of curved composite panels loaded into the postbuckling range. WEBSTER is a two-dimensional elasticity analysis for the skin-stiffener interface. This paper presents results of the predictive methodology. The entire analysis can be performed on a personal computer.

INTRODUCTION

Recent studies have indicated that the most common mode of failure for stiffened composite panels loaded into the postbuckling range is stiffener/skin separation. An assessment of the current postbuckled stiffened panel design, analysis, and application technology (References 1 and 2) shows that, for both static and fatigue loading, stiffener/skin separation consistently occurs at loads below other competing failure modes, such as skin compression failure and delamination. Because stiffener/skin separation is not accounted for in the existing design methodology, the application of existing postbuckling methodology to the design of advanced composite panels has resulted in unconservative designs. In order to fully realize the weight saving potential of postbuckled designs, this failure mode must be accounted for.

[1] This work was performed under NASA/Northrop Contract NAS1-18842, entitled "Innovative Composite Fuselage Structures."

Several attempts have been made in the last decade to predict the stiffener/skin separation of postbuckled, stiffened composite panels. These include semi-empirical models of References 1 and 3, strength of material models in References 4, 5, and 6, and elasticity models of References 7 and 8. In Reference 1, an empirical equation is derived by analogy with the crippling data for plates with one edge simply supported and one edge free. It is hypothesized that when the panel web strain reaches the crippling strain, the interfacial stresses become high enough to cause failure. The model proposed in Reference 3 is based on the hypothesis that skin/stiffener separation is caused by the interface normal stress induced by torsional stress in the stiffener. The average torsional stress in the stiffener, obtained from postbuckling analysis method of Reference 9 is empirically related to the bondline normal stress.

In Reference 4, a stiffener/skin delamination model was developed to determine the out-of-plane stresses in postbuckled stiffened shear panels. The physical behavior is simulated by a beam aligned parallel to the diagonal buckles through the point of maximum deflection. The Rayleigh-Ritz method was used to obtain the interfacial stresses. A similar model based on the large deflection beam theory was developed in References 5 and 6.

A three-dimensional analysis, based on the principle of virtual work was developed in Reference 7. The problem was formulated based on plate theory; continuity was enforced through the adhesive interface deformation. The problem was solved by the Galerkin method. Three out-of-plane stress components were obtained. A two-dimensional local elasticity model was used in Reference 8 to investigate the state of stress at the interface between a composite skin and the flanges of a cocured or secondarily bonded stiffened panel.

The preceding investigations examined the local response at the skin/stiffener interface. No attempts were made to relate the remote loading to the local response. In this paper, a methodology is developed that integrates the postbuckling analysis method of Reference 10 and the out-of-plane stress analysis model of References 8 and 11 into a single analysis package. The analytical approach and numerical results are presented in the following sections. The entire analysis can be performed on a personal computer.

ANALYSIS METHODOLOGY

The crux of the present methodology are two analysis packages: (1) PACL1, which predicts the stress and displacement fields in a stiffened postbuckled panel and (2) WEBSTER, which predicts the local interfacial (shear and normal) stresses at the skin and stiffener flange junction. PACL1 (Reference 10) is a Rayleigh-Ritz analysis of curved composite panels loaded into the postbuckling range under axial compression and shear loads. WEBSTER (Reference 11) is a two-dimensional elasticity analysis for the skin/stiffener interface. These analysis methods and the integrated methodology are briefly discussed in the following paragraphs.

PACL1. The energy approach was used to formulate the postbuckling problem in the PACL1 analysis package. The problem was formulated for a stiffened, curved anisotropic laminated plate. The laminate was assumed to be balanced and symmetric. A small imperfection in the lateral displacement was also included in the formulation. The panel geometry and the coordinate system are shown in **Figure 1**. This

figure also shows the relationship between the overall postbuckling structural configuration and the panel geometry used in the analysis. Since the adjacent bays are assumed to deform in an identical fashion, a single bay was analyzed. **Figure 1** shows that the material properties for the skin are A^*_{ij} and D^*_{ij}, where A^*_{ij} (A^*_{11}, A^*_{12}, A^*_{22}, and A^*_{66}) is the skin stiffness matrix and D^*_{ij} (D^*_{11}, D^*_{12}, D^*_{16}, D^*_{22}, D^*_{26}, and D^*_{66}) is the skin rigidity matrix. The material axes 1 and 2 are assumed to coincide with the panel geometry coordinate axes x and y, respectively. The panel, with length a and width b, is bounded by stringers along the straight edges and frames or rings along the curved edges. The cross-sectional area, Young's modulus and moment of inertia of the stringers are A_s, E_s, and I_s, respectively. Those of the frames are A_f, E_f, and I_f. The radius of the curved panel is R.

The energy expressions are written in terms of the displacement components u, v, and w in the x, y, and z directions, respectively. The panel is assumed fixed along x = o and subjected to a system of combined compression (N_x) and shear (N_{xy}) load along the edge x = a. The out-of-plane displacement (w) is assumed to be zero along all four edges.

The total potential energy, Π, is the sum of the strain energy stored in the skin, U_w, in the stringers, U_s, in the frames, U_f, and the potential of the external loads, Ω, and is written as

$$\Pi = U_w + U_s + U_f + \Omega \tag{1}$$

The strain energy in the skin for an anisotropic plate with $A^*_{16} = A^*_{26} = 0$ is given by

$$\begin{aligned} U_w = -\frac{1}{2}\int_v \{ & A^*_{11}\epsilon_x^2 + 2A^*_{12}\epsilon_x\epsilon_y + A^*_{22}\epsilon_y^2 + A^*_{66}\gamma_{xy}^2 \\ & + D^*_{11}w_{,xx}^2 + 2D^*_{12}w_{,xx}w_{,yy} + 4D^*_{16}w_{,xx}w_{,xy} \\ & + D^*_{22}w_{,yy}^2 + 4D^*_{26}w_{,yy}w_{,xy} + 4D^*_{66}w_{,xy}^2 \} \, dv \end{aligned} \tag{2}$$

where ϵ_x, ϵ_y, and γ_{xy} are the strain components. Commas denote differentiation with respect to the subscripted variables.

The strains are expressed in terms of the displacements u, v, and w using the nonlinear strain-displacement relations.

In the derivations that follow, the coordinate variables x and y are normalized with respect to their respective panel dimensions. The normalized coordinates (ξ, η) are given by

$$\xi = \frac{x}{a}, \quad \eta = \frac{y}{b} \tag{3}$$

The strain energy in the stringer is

$$U_s = \frac{A_s E_s}{2a}\int_o^1 u_\xi^2(\xi,0)\, d\xi + \frac{I_s E_s}{2a^3}\int_o^1 v_{\xi\xi}^2(\xi,0)\, d\xi \tag{4}$$

The strain energy in the frame is

$$U_F = \frac{A_f E_f}{2b} \int_o^1 v_\eta^2 (1,\eta)\, d\eta + \frac{I_f E_f}{2b^3} \int_o^1 u_{\eta\eta}^2 (1,\eta)\, d\eta \tag{5}$$

The potential of the external loads is

$$\Omega = -bN_{xx} \int_o^1 u(1,\eta)\, d\eta - bN_{xy} \int_o^1 v(1,\eta)\, d\eta \tag{6}$$

The solution method employs the principle of minimum potential energy. In applying the principle of minimum potential energy, the displacement components are assumed to be functions of the independent variables ξ and η. The selected functions must satisfy the displacement boundary conditions and minimize the total potential energy. A generalized series expression for the displacement functions with unknown coefficients was selected for the present analysis and they are as follows:

$$\begin{aligned} u &= A_{nm} f_1 + a_1 a\xi \\ v &= B_{nm} f_2 + b_1 a\xi \\ w &= C_{nm} f_3 + D_{nm} f_4 + w_o f_5, \end{aligned} \tag{7}$$

The coefficients A_{nm}, B_{nm}, C_{nm}, D_{nm}, a_1, and b_1 are unknown coefficients to be determined by minimizing the total potential energy. The term w_o in Equation 7 is the initial imperfection at the panel center. The function $f_5 = f_5(\xi,\eta)$ is the initial imperfection function in terms of the lateral displacement and satisfies the displacement boundary conditions.

The total potential energy is minimized with respect to the unknown coefficients. The minimization process yields a system of nonlinear algebraic equations. Details of these algebraic equations are given in Reference 10. These equations can be expressed in the following form:

$$\left[\frac{\partial \pi}{\partial A} \bigg|_L \right] = \left[\frac{\partial \pi}{\partial A} \bigg|_N - C \right] \tag{8}$$

where the subscript L denotes the linear terms of the partial derivative of the total potential energy with respect to a particular unknown coefficient (A), subscript N denotes the nonlinear terms and C represents the terms that are independent of the unknown coefficients.

The number of nonlinear algebraic equations in the system given by Equation 8 depend on the number of buckling modes used in the analysis. The number of equations can be calculated from the relation 4NM+2, where N is the number of buckling modes in the x-direction and M is the number of buckling modes in the y-direction. As N and M increase, the number of nonlinear terms on the right-hand side of Equation 8 also significantly increases. A large number of nonlinear terms present numerical difficulty in solving Equation 8. On the other hand, although the postbuckling behavior of a stiffened panel is mixed-mode behavior in general, the displacement response is dominated by a single buckling mode. Therefore, if the dominant buckling

mode is known, the postbuckling behavior can be accurately described using a single-mode analysis.

In addition, for the case of no initial imperfection, i.e., $w_o = o$, the total number of integrals involved in Equation 8 is reduced to 108. The reduced system of nonlinear equations can be solved with very high accuracy by an iterative technique using the method of successive linearization. In this method, each of the unknown coefficient, A_{nm}, B_{nm}, C_{nm}, D_{nm}, a_1, and b_1 is assigned an initial value and substituted into the right-hand-side of Equation 8. Equation now becomes a system of linear algebraic equations and can be easily solved for the new values of the unknown coefficients. Using the new set of coefficients as initial values, another set of improved coefficients can be obtained by solving the linearized system. This procedure is continued until the solution converges within a desired limit. In the actual solution, only the initial values of the coefficients at the first load level need to be assigned. At higher load levels, the initial values are obtained by extrapolating the converged solutions of the preceding load levels to reduce the number of iterations. This numerical procedure for single mode analysis was coded in the PACL1 computer program.

WEBSTER. This analysis is a generalization of the elasticity method used in References 8 and 12. The method models the stiffener flange and the adjacent structure (skin) as separate orthotropic plates that are bonded together with a bondline of zero thickness. Each plate may have different mechanical properties.

The local model considers a flange terminating at the skin, as shown in Figure 2. The problem is formulated as a generalized plane deformation problem (i.e., the stress and strain components are independent of the z-coordinates).

The stress-strain relations are given by

$$\epsilon_i = a_{ik}\sigma_k \qquad i,k = 1,2,3,4,5,6 \tag{9}$$

and

$$a_{ik} = 0 \qquad \text{if } i \neq k \text{ for } i,k = 4,5,6$$

where a_{ik} are the components of the effective compliance matrix. The equilibrium equations are satisfied automatically by defining the stress functions

$$\sigma_x = \frac{\partial^2 F}{\partial y^2}, \quad \sigma_y = \frac{\partial^2 F}{\partial x^2}, \quad \tau_{xy} = -\frac{\partial^2 F}{\partial x \partial y} \tag{10}$$

The equations governing the stress function (F) are derived from the stress-strain relations (Equation 9) and the linear strain displacement relations. The governing equation becomes

$$\beta_{22}\frac{\partial^4 F}{\partial x^4} + (2\beta_{12} + \beta_{66})\frac{\partial^4 F}{\partial x^2 \partial y^2} + \beta_{11}\frac{\partial^4 F}{\partial y^4} = 0 \tag{11}$$

where

$$\beta_{ij} = a_{ij} - \frac{a_{i3}a_{j3}}{a_{33}}, \quad i=1,2,4,5,6 \tag{12}$$

The homogeneous solution of Equation 11 can be approximated by a series expansion in terms of complex variables, defined as $Z = x + \mu y$. The stress functions are assumed to be functions of the complex variables, specifically $F = F(Z)$. The governing equation becomes

$$[\beta_{22} + \mu^2(2\beta_{12} + \beta_{66}) + \mu^4\beta_{11}]\ F^{iv}(Z) = 0 \tag{13}$$

Thus, μ, depending on material properties, are the roots of the characteristic equation

$$\beta_{22} + \mu^2(2\beta_{12} + \beta_{66}) + \mu^4\beta_{11} = 0 \tag{14}$$

The displacements can then be expressed in terms of the stress functions as

$$\begin{aligned} u &= (\mu_k^2\,\beta_{11} + \beta_{12})\ F'(Z_k) \\ v &= \frac{1}{\mu_k}(\mu_k^2\,\beta_{12} + \beta_{22})\ F'(Z_k) \end{aligned} \tag{15}$$

where, μ_k (k = 1,2,3,4) is the kth root of Equation 14.

The series expressions for the stress functions are then stated as

$$F(Z) = \sum_{i}^{N} C_i \sum_{k=1}^{4} \alpha_{ik} \frac{Z_k^{\lambda+2}}{(\lambda+1)(\lambda+2)} \tag{16}$$

where, C_i are constants to be determined. The stresses and displacements can then be expressed in terms of the constants C_i and the complex variables Z_k.

The constants $\alpha_k^{(i)}$ are determined by satisfying prescribed boundary conditions. The boundary conditions include zero stress along the free edges, and stress and displacement continuity conditions along the interface. These conditions are satisfied by expressing the stress and displacement components in polar coordinates (r,θ). It should be noted that Equations 9 through 16 are derived for the skin and the flange, such that each one actually represents two equations.

The following relations use the subscript (or superscript) 1 and 2 to denote the flange and the skin, respectively. Surfaces AB and FA are assumed to be stress free. These boundary conditions are stated respectively as

$$\sigma_\theta^{(1)}(r,\beta) = \tau_{r\theta}^{(1)}(r,\beta) = 0 \tag{17}$$

$$\sigma_\theta^{(2)}(r,-\pi) = \tau_{r\theta}^{(1)}(r,-\pi) = 0 \tag{18}$$

The bond between the flange and the skin is assumed to be ideal along the interface (i.e., the stresses and displacements along this line are continuous). The stress continuity conditions at the interface are stated as

$$\sigma_\theta^{(1)}(r,0) = \sigma_\theta^{(2)}(r,0) \tag{19}$$

$$\tau_{r\theta}^{(1)}(r,0) = \tau_{r\theta}^{(2)}(r,0) \tag{20}$$

The displacement continuity conditions at the interface are

$$u^{(1)}(r,0) = u^{(2)}(r,0) \tag{21}$$

$$v^{(1)}(r,0) = v^{(2)}(r,0) \tag{22}$$

A system of eight homogeneous equations in terms of the eight unknown constants α^i_k (i=1,2 and k=1,2,3,4) result when the stress and displacement expressions are substituted into the boundary condition relations, Equations 17 through 22.

Global analysis of the structure provides the forces that are applied to surfaces CD and EF of the local region shown in **Figure 2**. Surfaces FA, AB, and BC are stress free. The overall applied force system must satisfy the equilibrium condition of the local region ABCDEF. WEBSTER solves this problem using boundary collocation with collocation points distributed along edges CD and EF.

PACSTER. PACSTER is an integrated analysis package that utilizes the displacement field obtained from the PACL1 analysis to determine the interfacial stresses at the skin/stiffener junctions by performing WEBSTER analysis. Therefore, the stress formulation in WEBSTER must be modified. The displacements in the local (WEBSTER) coordinates system can be expressed in terms of the stress function (F(Z)) as given by Equation 15. This modification essentially changed the original prescribed boundary force problem of WEBSTER into a prescribed boundary displacement problem. The displacement field obtained from PACL1 analysis is then used as boundary displacements in the WEBSTER analysis. This procedure has been automated and resulted in the present computer code PACSTER, which is operational on a 286/386 computer.

A flowchart detailing the logic of the analysis methodology is shown in **Figure 3**. The program requires material properties, panel geometry, sectional properties of the stringers and the frames and the load parameters as input. Following input execution of PACL1 begins and the program calculates the displacement field of the entire panel. The displacements are then screened to identify critical locations. Because the objective of this analysis is to determine the applied load at which skin/stiffener separation occurs, the critical locations are selected based on the maximum displacements in the vicinity of the stringer or the frame. A total of four critical locations are selected for WEBSTER analysis. They are selected based on critical v and w displacements near the stringers and critical u and w displacements near the frames. After the critical locations are identified, the program proceeds to transfer all the required data into the local coordinate system for the WEBSTER analysis. The displacements associated with the critical locations are used as boundary conditions for the interfacial stress calculations. WEBSTER is executed four times for the four critical locations identified.

The interlaminar normal and shear stresses obtained from the local analysis are then used in the failure analysis. The failure criterion currently used in PACSTER is an average stress criterion in a quadratic form. The average stress criterion suggested in Reference 13 is applied here. The average shear (τ_{ave}) and normal (σ_{ave}) stresses over a characteristic length (a_o) are computed, and failure is defined as

$$F_I = \left[\left(\frac{\tau_{ave}}{\tau_o} \right)^2 + \left(\frac{\sigma_{ave}}{\sigma_o} \right)^2 \right]^{1/2} \geq 1 \qquad (23)$$

where, τ_o and σ_o are shear and normal strength of the interface material, respectively.

The procedure described above is repeated for each load increment until the prescribed maximum load is reached.

Figure 4 illustrates the typical critical location selection procedure. A curved panel enclosed with stiffeners and frames is considered. The stiffener flange is of length a_s and the frame flange is of length b_f. In-plane compression and shear forces are applied to the curved panel. The resulting displacement pattern obtained from PACL1 analysis is shown in **Figure 4**. For the skin/stiffener separation analyses, the region of significance is highlighted in the figure. From the displacement field, the program has identified S_{cz} and F_{cz} as critical locations. The out-of-plane stress distributions along the skin/stiffener interface at location S_{cz} are shown in **Figure 5**. This figure indicates high stress concentrations, both normal and shear, occur at the junction of the skin and the stiffener. These stress concentrations contribute to the skin/stiffener separation failure of the panel.

NUMERICAL EXAMPLE

A curved panel tested in Reference 10 is selected as an example to illustrate the analysis procedure. The composite panel is 24 inches long, 12.2 inches wide with a radius of 45 inches. The panel skin is made of A370-5H/3501-6 woven graphite/epoxy and AS/3501-6 unidirectional graphite/epoxy. The material properties, skin layup, and stiffener configurations are shown in **Figure 6**. The flange of the frame has a layup of $[\underline{45}_2/90_2/0/90_2/\underline{45}_2]$. The panel is under axial compression with total load P_x. The interfacial strengths are assumed to be σ_o=3000 psi and τ_o=11000 psi. These allowables are typical of the values obtained from flatwise tension and short beam shear tests, respectively.

The results of the PACSTER analysis are shown in **Figure 7**. The critical locations identified by the program are shown in the upper-left corner of the figure. They are denoted by (1) v-s/s: critical skin/stiffener interface due to v-displacement; (2) w-s/s: critical skin/stiffener interface due to w-displacement; (3) u-s/f: critical skin/frame interface due to u-displacement; and (4) w-s/f critical skin/frame interface due to w-displacement. As shown in the figure, these locations depend on the applied load level.

The interfacial stresses are expressed in terms of the failure index (F_I) defined in Equation 23. **Figure 7** shows that the most critical location is w-s/s. At this location, F_I = 1.0 when the total compression reaches 9100 lb. That is

skin/stiffener separation failure will be initiated at the location w-s/s at 9100 lb of axial compression. Test results in Reference 10 showed the initial buckling occurred at 325 lb/in or approximately 4000 lb, and final failure of the panel, by skin/stiffener separation, at 825 lb/in or 10,050 lb. The results in **Figure 7** show that PACSTER under-predicts the final failure by approximately 10 percent. This may be due to the conservative estimate of the interfacial strengths (σ_o and τ_o) or the uncertainty in the out-of-plane properties of the materials.

SUMMARY

A methodology has been developed to predict the failure of postbuckled, stiffened composite panels by skin/stiffener separation. The methodology is applicable to curved as well as flat panels under combined uniaxial compression and in-plane shear loads. The entire analysis can be performed on a personal computer.

Limited correlation of analytical predictions with experimental data indicated that the analysis provided reasonable prediction of failure load. Further data correlation is necessary to validate the methodology.

REFERENCES

1. Deo, R. B., Agarwal, B. L., and Madenci, E., "Design Methodology and Life Analysis of Metal and Composite Panels," AFWAL-TR-85-3096, Final Report, Volume I, Contract F33615-81-C-3208, December 1985.

2. Deo, R. B. and Madenci, E., "Design Development and Durability Validation of Postbuckled Composite and Metal Panels," AFWAL-TR-85-3077, Final Report, Technology Assessment, Contract F33615-84-C-3220, May 1985.

3. Arnold, R. R., "Disbond Criterion for Postbuckled Composite Panels," AIAA-CP-87-0732, presented at the 28th AIAA/ASME/ASCE/AHS SDM Conference, Monterey, CA, April 6-8, 1987.

4. Agarwal, B. L., "A Model to Simulate Failure Due to Stiffener/Web Separations of Composite Tension Field Panels," AIAA-CP-82-0746, presented at the 23rd AIAA/ASME/ASCE/AHS SDM Conference, New Orleans, LA, May 10-12, 1982.

5. Tsai, H. C., "Solution Method for Stiffener-Skin Separation in Composite Tension Field Panel," Report No. NADC-82171-60, October 1982.

6. Tsai, H. C., "Approximate Solution for Skin/Stiffener Separation Including Effect of Interfacial Shear Stiffness in Composite Tension Field Panel," Report No. NADC-83131-60, November 1983.

7. Wang, J. T. S. and Biggers, S. B., "Skin/Stiffener Interface Stresses in Composite Stiffened Panels," NASA Contract Report No. 172261, January 1984.

8. Hyer, M. W. and Cohen, D., "Calculation of Stresses and Forces Between the Skin and Stiffener in Composite Panels," AIAA-CP-87-0731, presented at the 28th AIAA/ASME/ASCE/AHS SDM Conference, Monterey, CA, April 6-8, 1987.

9. Arnold, R. R. and Meyers, J., "Buckling, Postbuckling, and Crippling of Materially Nonlinear Laminated Composite Plates," International Journal of Solids and Structures, Volume 20, No. 9 and 10, pp 863-880, 1984.

10. Deo, R. B., Kan, H. P., and Bhatia, N. M., "Design Development and Durability Validation of Postbuckled Composite and Metal Panels, Volume III - Analysis and Test Results," WRDC-TR-89-3030, Final Report, Contract F33615-84-C-3220, November 1989.

11. Paul, P. C., Saff, C. R., Sanger, K. B., Mahler, M. A., Kan, H. P., and Deo, R. B., "Out-of-Plane Analysis for Composite Structures," Volumes I and II, Final Report, NADC Contract N62269-87-C-0226, August 1989.

12. Wang, S. A. and Choi, I., "Boundary Layer Effects in Composite Laminates," Part I and II, Journal of Applied Mechanics, Volume 49, No. 3, pp 541-560, 1982.

13. Whitney, J. M. and Nuismer, R. J., "Stress Fracture Criteria for Laminated Composites Containing Stress Concentrations," Journal of Composite Materials, Volume 8, 1974, pp 253-265.

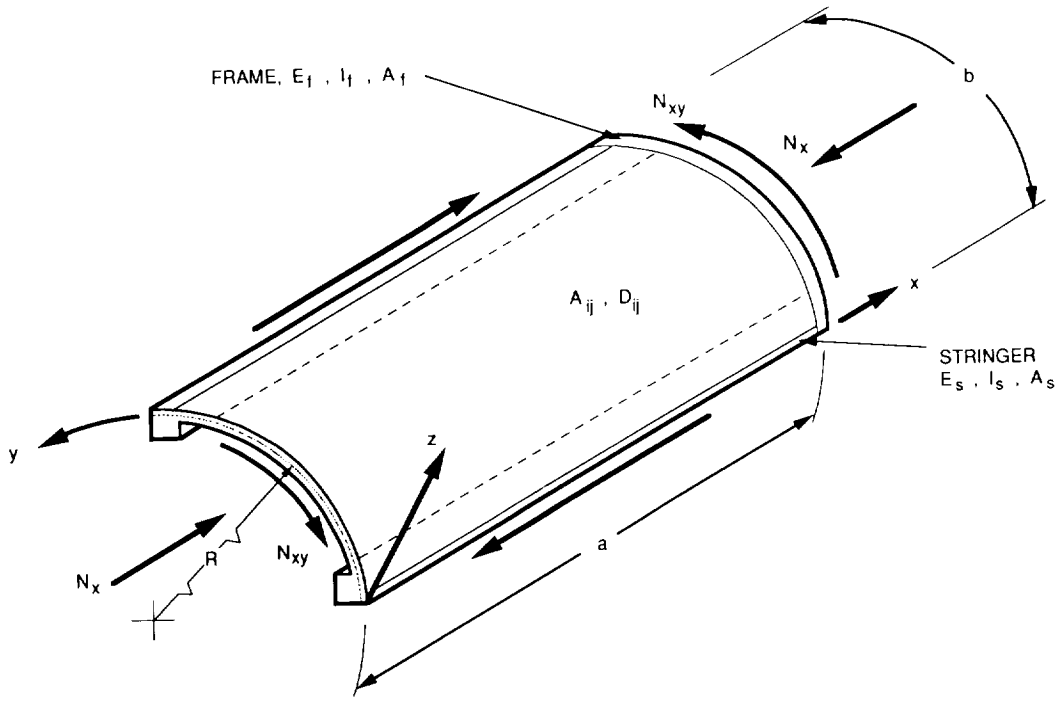

Figure 1. Curved Panel Geometry and Coordinate System Used in PACLI Analysis.

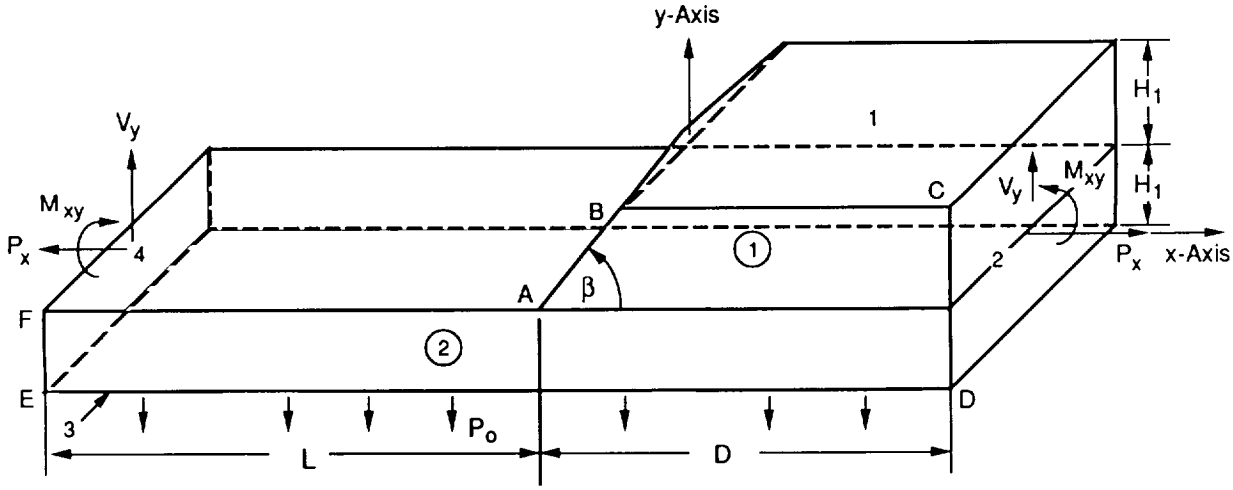

Figure 2. Local Elasticity Model for WEBSTER Analysis.

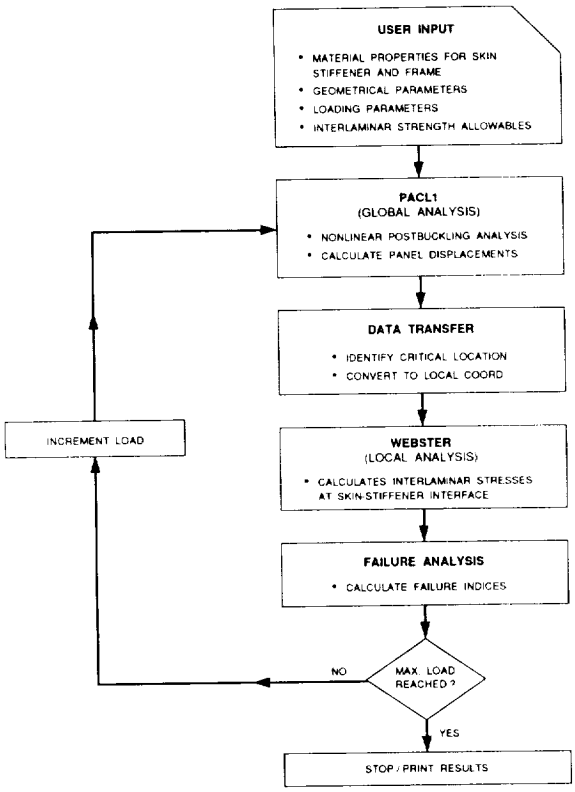

Figure 3. Flowchart for Analysis of Skin-Stiffener Separation in Postbuckled Panels.

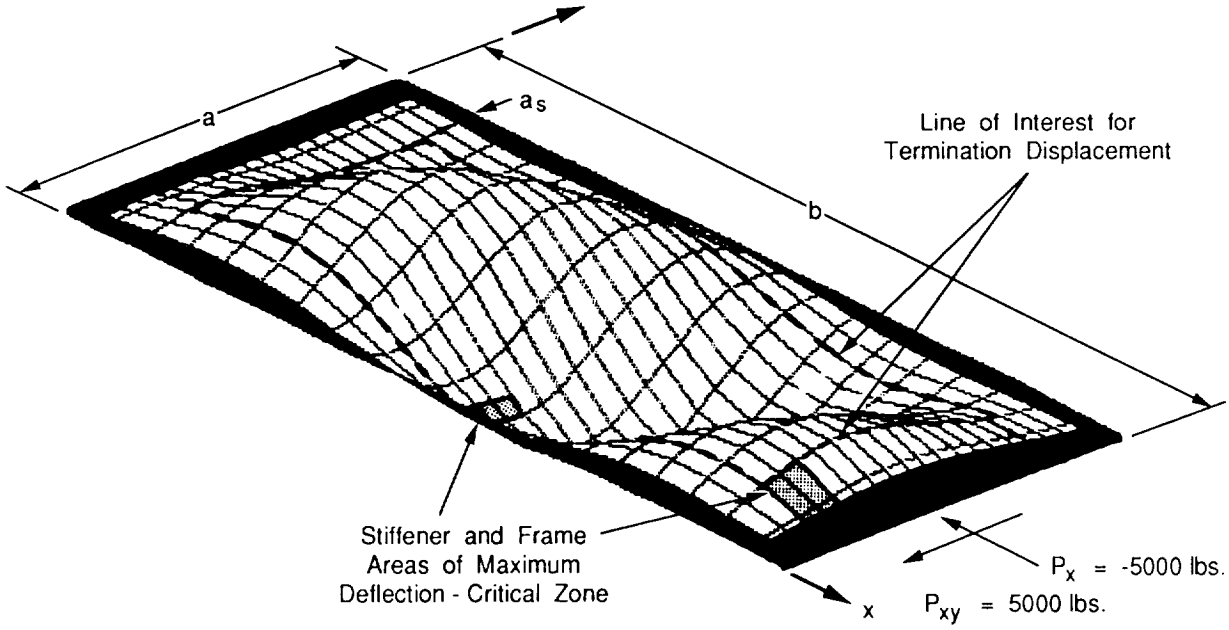

Figure 4. Postbuckled Panel With Stiffener Termination Details.

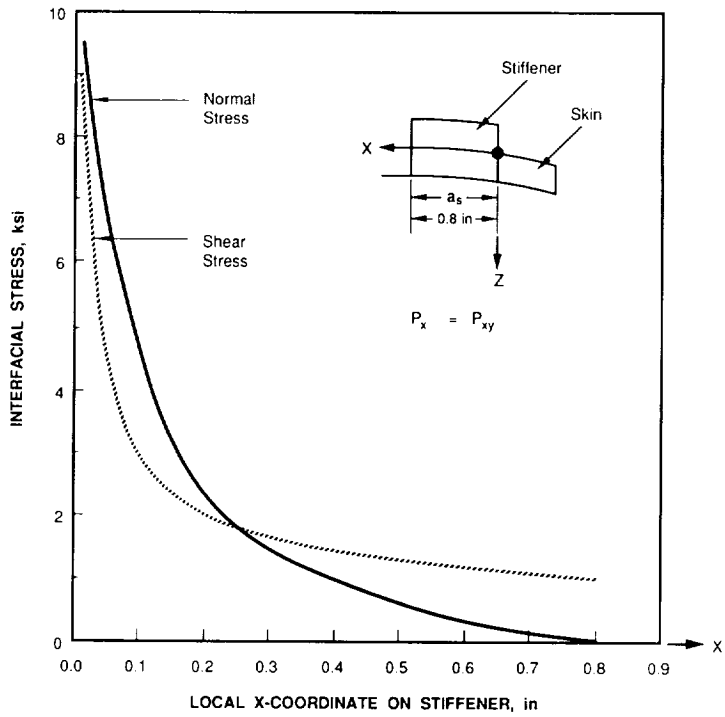

Figure 5, Interlaminar Stress Distribution at Stiffener Termination in Stiffener Critical Zone.

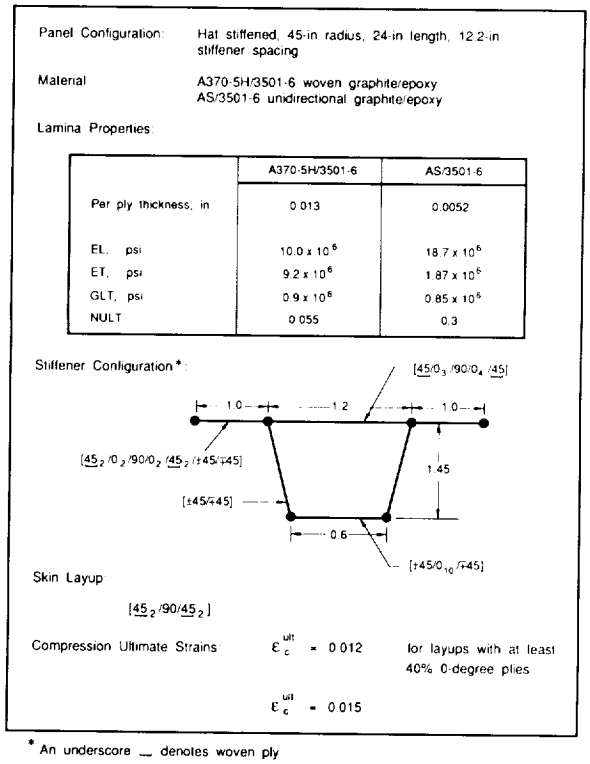

Figure 6. Example Problem Data for Program PACSTER.

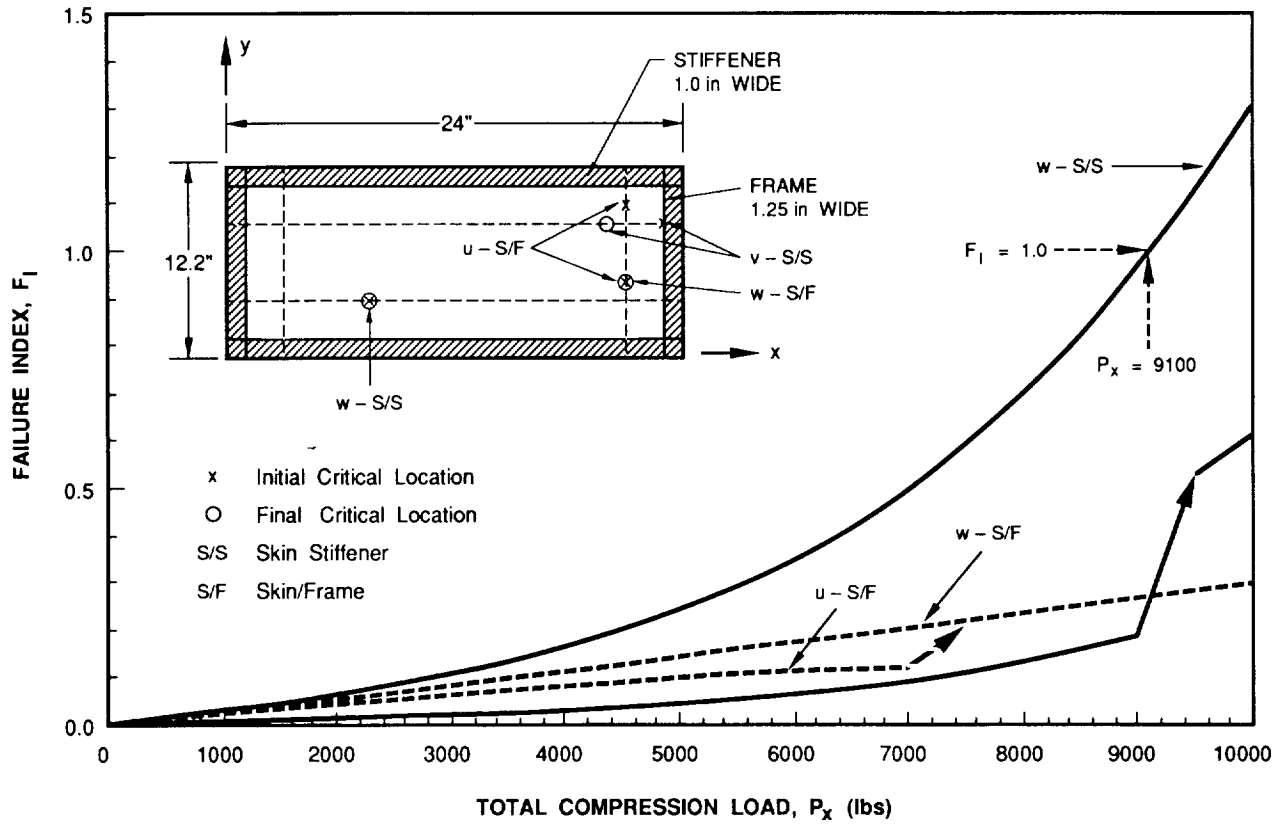

Figure 7. Analytical Results of the Example Problem.